

# 14 Lacertae: A case of shell-orbit coupling?\*

M. Bossi<sup>1</sup>, N.S. Nuñez<sup>1,2</sup>, G. Guerrero<sup>1</sup>, J.-P. Sareyan<sup>3</sup>, and M. Alvarez<sup>4</sup>

<sup>1</sup> Osservatorio Astronomico di Brera, Via Bianchi 46, I-22055 Merate LC, Italy

<sup>2</sup> Observatorio Astronómico P. Buenaventura Suarez, C.C. 1129, Asunción, Paraguay

<sup>3</sup> Observatoire de la Côte d'Azur, BP. 139, F-06003 Nice Cedex, France

<sup>4</sup> Observatorio Astronómico Nacional, UNAM, Apdo. 877, Ensenada, B.C. 22800, Mexico

Received November 6, 1996; accepted June 5, 1997

**Abstract.** We present new photometric and spectroscopic observations of this peculiar Be star: respectively 516  $\Delta V$  values in 16 nights and 50 spectrograms in 4 nights in the H $\alpha$  region. A feature of the HeI $\lambda 6678$  line profile seems to indicate the presence of a double-lined binary spectrum. Nevertheless, an analysis of our and other available data (former published and unpublished photometry) leads us to rule out the current interpretations of the double-wave light curve shown by this star: 14 Lac can neither be identified as an ellipsoidal variable nor as an eclipsing binary. Its variability is likely to be produced in the circumstellar region by a shell distortion due to the presence of the companion star, even if there is not enough evidence to exclude other hypotheses. The implications both of the duplicity assumption and of its possible refutation are discussed.

**Key words:** stars: emission-line, Be — general; spectroscopie (stars:) binaries: — stars: individual: 14 Lac

## 1. Introduction

The Be star 14 Lac (HD 216200) holds our attention since it shows on unusual time scales a variability pattern which is fairly common among these objects.

Slettebak (1982) classifies it as a B4 III star; Uesugi & Fukuda (1982) assign to its spectral lines a Doppler broadening  $v \sin i = 220$  km s $^{-1}$ ; Goraya & Gurm (1987) get, through their continuum spectrophotometry, an estimate of its temperature and gravity:  $T_{\text{eff}} = 18000$  K;  $\log g = 4.0$ .

*Send offprint requests to:* M. Bossi. Internet:  
bossi@merate.mi.astro.it

\* This work was partially supported by CNR and CONACYT in the ambit of their convention about scientific and technological collaboration.

In 1950–51 Walker (1952), using this object as a comparison star in his differential photometry of 16 Lac, observed a light variability on a time scale of days. Andrews (1968) suspected it of being a Be star from a comparison of photometric indices. The first spectroscopic evidence of this fact is due to Wackerling (1970), which observed a weak emission in H $\alpha$ .

The evaluations of the possible period or pseudoperiod of the light variations range from the  $\sim 20$  days of Hill et al. (1976) to the  $\sim 5$  days of Mantegazza (1980). Due to these time scales, and to the apparent non-sinusoidal shape of the light curve, the variability shown by 14 Lac has been generally ascribed to a tidal strain produced by the presence of a companion star. In an annual report from the Dominion Astrophysical Observatory (Richardson 1977) we find a trace of a spectroscopic study performed by G. Hill, which seemed to show evidence of a double-lined binary system with a period of  $\sim 10$  days. Unfortunately, this work has never been published. A quotation of Hill's spectroscopy in Pavlovski et al. (1994) makes up for that gap: combining the above quoted observations with their archive photometry, these authors seem now to raise 14 Lac from the rank of ellipsoidal variable to the one of eclipsing binary, giving for its period the value of 10 $^{d}085$ . More details are going to appear in a publication announced in that note.

Since the position of 14 Lac in the sky is close to the one of o And, we took advantage of an observational campaign on this well-known Be star organized in 1992 including also 14 Lac in our program. The photometric and spectroscopic data obtained on that occasion, combined with a re-analysis of the previous available photometry, allowed us to reach some conclusions presented in this paper.

## 2. Photometry

Three available sets of photometric data turned out useful for our work.

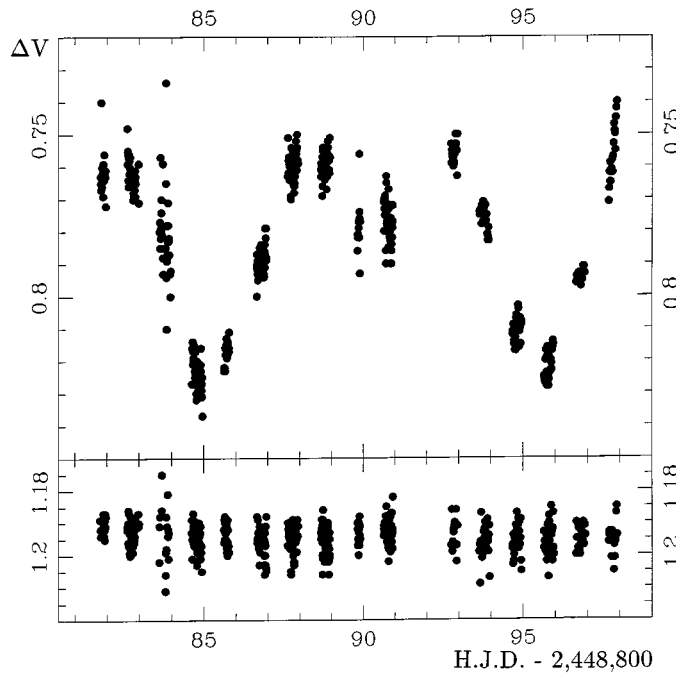


**Fig. 1.** The light curve resulting from our observations of 1992: the magnitude difference 14 Lac - 2 And (top) is compared, in the same scale, to the difference between the comparison magnitudes HD 217101 - 2 And (bottom)

– The 516  $\Delta V$  values (in the instrumental *UBV* system) obtained by us at the *Observatorio Astronómico Nacional* (San Pedro Martir, BC, Mexico) during the above quoted campaign (September 1992). These differential measurements were performed using the 0.84 m telescope equipped with a photon counting photometer; the light detector was a dry ice cooled GaAs phototube and the adopted *V* filter was made up of two elements (2 mm GG595 + 2 mm BG18). The data have not been transformed to Johnson's system since, in view of the complex variability pattern expected in o And, we preferred to increase our time coverage rather than to spend time in observing standard stars. As comparison stars (in common with o And) we used 2 And, HD 217101 and 10 Lac; all the magnitude differences are given with respect to the reference star 2 And. Our large set of data allowed us, in order to do it, to shift all our comparison objects to the same fictitious magnitude with great accuracy. The light stability of these stars has been checked also removing them by turns from the data files: such tests resulted all in increasing the variance of the light curves of o And and 14 Lac. Considering the size of our observational field (10 Lac is about  $8^\circ$  to the SW of 2 And), the data have been processed using the technique developed by Poretti & Zerbi (1993) in order to deal with the variations in extinction coefficient during each night. The

resulting light curve is shown in Fig. 1, interested people can get it in electronic form.

- The light curves in the DAO photometric system published in Hill et al. (1976), defined by 72 differential measurements in each of the filters (35), (44) and (55), comparable to the *U*, *B* and *V* standard ones respectively.
- The *UBV* photometry performed from August to November 1969 at the Astrophysical Station of Serra La Nave (CT, Italy) of the *Osservatorio Astronomico di Catania* by M. Rodonò, processed by L. Mantegazza and mentioned in Mantegazza (1980). These observations (Mantegazza 1995) consist of 210  $\Delta U$ , 188  $\Delta B$  and 192  $\Delta V$  values.

The basic information about these light curves is presented in Table 1, where the white noise contained in each time series has been evaluated from the root-mean-square difference between closely consecutive data. The corresponding signal-to-noise ratio, obtained assuming this white noise value as representative of the whole noise, is given in decibels: fans of the classical astronomical units are reminded that  $1 \text{ dB} = -0^m 25$ .

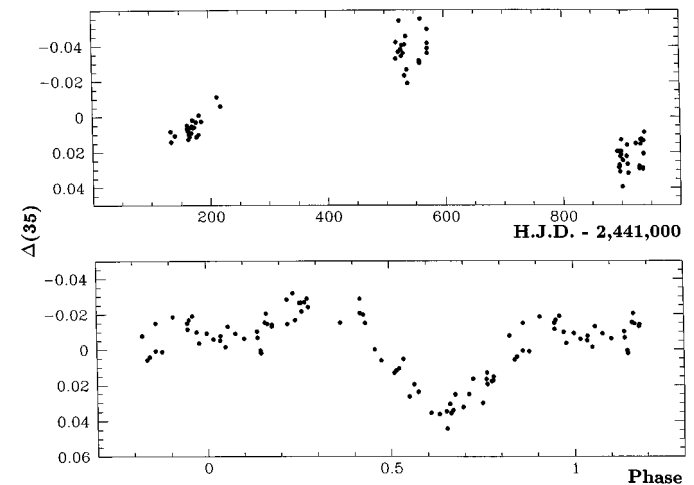


**Fig. 2.** Non-periodic (top) and periodic (bottom) component of the ultraviolet light curve published by Hill et al. (1976) resolved by the LIN algorithm (Bossi & La Franceschina 1995). The periodic term is phased with a frequency of  $0.09916 \text{ d}^{-1}$

Working on the assumption of simple periodic variations, first of all we have to determine their frequencies in the different epochs. So all the light curves, except the  $\Delta(35)$  series published by Hill et al. (1976), have been analyzed with this object using the PDM method (Stellingwerf 1978): this procedure is our most effective tool for analysing highly non-sinusoidal periodicities. Hill's ultraviolet curve, which presents a combination of a strongly non-sinusoidal periodic component with a long term trend, has been subjected to a MPDM

**Table 1.** Basic information about the available light curves examined in this work

	1969			1971-1973			1992
	$\Delta U$	$\Delta B$	$\Delta V$	$\Delta(35)$	$\Delta(44)$	$\Delta(55)$	$\Delta V$
No of measurements	210	188	192		72		516
No of nights		32			57		16
Total useful obs. time (hours)	86	76	70		48		102
Baseline (days)	120	120	103		805		16
Standard Deviation (mmag)	29.0	27.3	25.6	35.7	18.0	21.8	24.3
White Noise (mmag)	14.6	15.9	7.4	9.1	5.2	4.6	4.7
S/N ratio (dB)	4.7	2.8	10.4	11.6	10.4	13.2	14.1

**Table 2.** Frequencies, determined through the PDM (Stellingwerf 1978) and MPDM (Bossi & La Franceschina 1995) methods, of the non-sinusoidal periodic component observed in the light variations of 14 Lac at different epochs

Epoch	$U$ or DAO(35) Freq. ( $d^{-1}$ )	$B$ or DAO(44) Freq. ( $d^{-1}$ )	$V$ or DAO(55) Freq. ( $d^{-1}$ )
1969	$0.0991 \pm 0.0003$	$0.0995 \pm 0.0003$	$0.0995 \pm 0.0002$
1971 - 1973	$0.09916 \pm 0.00004$	$0.09920 \pm 0.00004$	$0.09918 \pm 0.00003$
1992			$0.0982 \pm 0.0003$

analysis (Bossi & La Franceschina 1995). As shown in Fig. 2, the LIN algorithm, presented in the quoted paper, has been able to resolve this time series into a non-periodic component and a periodic one with a frequency of  $0.09916 d^{-1}$ . The results are summarized in Table 2 and shown in Fig. 3. The errors have been determined by means of the standard statistical approach assuming each time series to consist of a periodic part (with the addition of a long term trend in the case of  $\Delta(35)$ ), described by a derived mean curve, and white noise. It is easy to verify the consistency of the frequencies derived from simultaneous observations at different wavelengths, while this frequency may or may not be constant at different times: the difference between the value obtained from the yellow curve of Hill et al. (1976) and the one derived from our  $V$  curve corresponds to more than  $3\sigma$ . The significance of this gap depends on the just quoted assumption of simple periodic signals.

A stronger evidence supports the presence of changes in amplitude and shape of the light patterns with timescales of years.

We can describe effectively some features of this evolution by means of a Fourier decomposition of the examined light curves, assumed, in each of the three observational

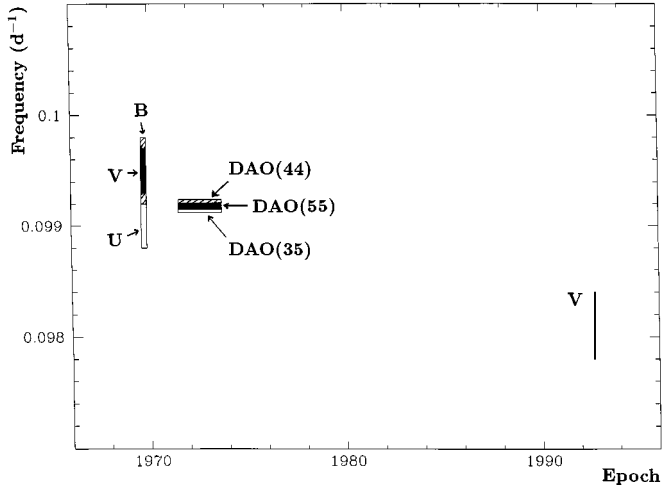
epochs, to be periodic with the previously determined frequency. In all seven time series, the basic frequency and its first harmonic appear enough to represent the periodic component of the signal. In Table 3 we show the behaviour of three meaningful parameters: their combined standard deviation  $\sigma_{1+2} = (\frac{1}{2}a_1^2 + \frac{1}{2}a_2^2)^{\frac{1}{2}}$ , their amplitude ratio  $a_2/a_1$  and their phase difference  $\phi_{21} = \phi_2 - 2\phi_1$  (for the last definition see e.g. Simon & Lee 1981).

The growth of  $\sigma_{1+2}$  resulting from the first line of the table cannot be considered as an evidence of amplitude changes: the observed amplitude of the light variations is a wavelength-sensitive parameter (we can observe a greater variability in the yellow and ultraviolet measurements than in the blue ones) and the examined sets of data were produced in different epochs by means of different equipments. Nevertheless, it is interesting to compare this pattern with the observations performed in 1980 and 1981 by Garrido et al. (1983), which found no significant variation of the magnitude of this star.

The changes in the shape of the yellow ( $V$  or DAO(55)) light curve, described by  $a_2/a_1$  and  $\phi_{21}$ , are shown in Fig. 4, where the amplitude ratio and the phase difference are represented in polar co-ordinates with the respective errors. As we can verify observing Table 3, this behaviour,

**Table 3.** Evolution of some parameters derived from the Fourier decomposition of the light curves

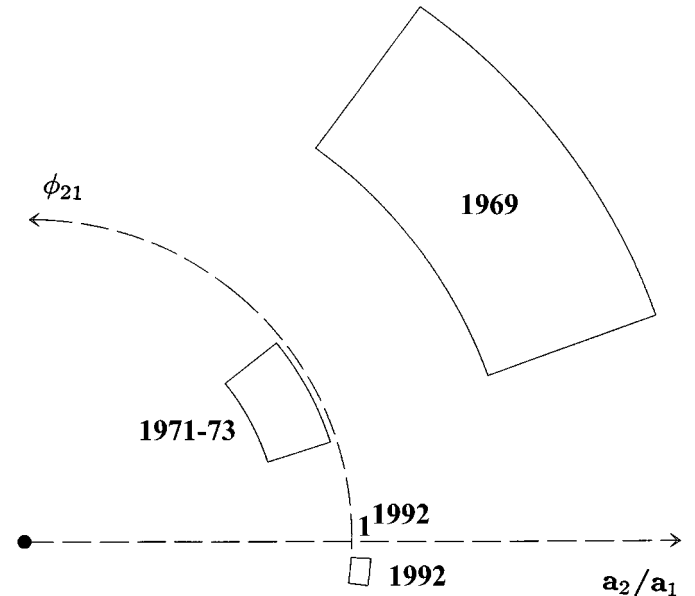
	Band	1969	1971 - 1973	1992
$\sigma_{1+2}$	V or DAO(55)	$0.^m0184 \pm .0011$	$0.^m0197 \pm .0011$	$0.^m0218 \pm .0003$
	B or DAO(44)	$0.^m0159 \pm .0015$	$0.^m0145 \pm .0013$	
	U or DAO(35)	$0.^m0178 \pm .0015$	$0.^m0195 \pm .0007$	
$a_2/a_1$	V or DAO(55)	$1.77 \pm .27$	$0.88 \pm .10$	$1.03 \pm .03$
	B or DAO(44)	$1.85 \pm .46$	$0.76 \pm .15$	
	U or DAO(35)	$2.21 \pm .51$	$0.64 \pm .05$	
$\phi_{21}$	V or DAO(55)	$0.65 \pm .30$	$0.50 \pm .18$	$-0.09 \pm .04$
	B or DAO(44)	$0.74 \pm .45$	$0.63 \pm .28$	
	U or DAO(35)	$0.52 \pm .42$	$0.52 \pm .11$	

**Fig. 3.** Frequencies of the non-sinusoidal periodic component observed in the light variations at different epochs. The length of the rectangles represents the duration of the observational seasons, the height the error bar on the frequency values

unlike the amplitude of the light curve, shows no significant dependence on the wavelength.

Further information is given by a frequency analysis of the magnitude changes performed dropping the monoperiodic restriction. The results, obtained using Vanicek's (1971) method and adjusting the outcomes by means of a simultaneous nonlinear least squares fit, are synthesized in Table 4. The values relative to the DAO(35) curve result from simultaneous fits, optional in Vanicek's algorithm, with a cubic polynomial, describing the above quoted long term trend, in addition to the sinusoids.

The scanned frequency range ( $0 - 10 \text{ d}^{-1}$ ) allows us to exclude the presence, in all the available sets of photometric data, of detectable rapid changes besides the

**Fig. 4.** Values of the amplitude ratio and of the phase difference between the basic frequency and its first harmonic resulting from the Fourier decomposition of the V and DAO(550) light curves represented in polar co-ordinates ( $a_2/a_1 \equiv \rho$ ;  $\phi_{21} \equiv \theta$ )

well-known light variations on a time scale of days: just this time scale, rather than its quite common variability pattern (see e.g. Balona et al. 1987, or van Vuuren et al. 1988), characterizes this interesting Be star.

Moreover, a cross-check of the frequency spectrum of our mexican data against the one, obtained through the same procedure, of the light variations simultaneously detected in o And reassured us once again about the

**Table 4.** Frequencies detected in the light curves using Vanicek's method and adjusted by means of a simultaneous nonlinear least squares fit

Epoch	Band	Frequencies ( $\text{d}^{-1}$ )		
		$\nu_1$	$\nu_2$	$\nu_3$
1969	<i>U</i>		$0.1991 \pm .0004$	$0.3083 \pm .0004$
	<i>B</i>		$0.1996 \pm .0005$	$0.3083 \pm .0004$
	<i>V</i>		$0.1998 \pm .0003$	$0.3069 \pm .0006$
1971-1973	DAO(35)	$0.09916 \pm .00005$	$0.19835 \pm .00005$	
	DAO(44)	$0.09920 \pm .00006$	$0.19834 \pm .00008$	
	DAO(55)	$0.09916 \pm .00004$	$0.19835 \pm .00005$	
1992	<i>V</i>	$0.0974 \pm .0008$	$0.1971 \pm .0008$	

constancy of our comparison stars: no common periodicity has been detected in both time series.

Finally, the data obtained in 1969 hold in particular our attention. Their interest, besides the appearance of a  $\nu_3 \simeq 3\nu_1$  frequency instead of the basic one, lies in the ratio of this frequency to  $\nu_2$ :  $1.548 \pm .004$ ,  $1.545 \pm .004$  and  $1.536 \pm .004$  respectively in the *U*, *B* and *V* bands. The differences between these values and  $3/2$ , corresponding to  $12\sigma$ , more than  $11\sigma$  and  $9\sigma$  respectively, are meaningful without doubt. Therefore, we cannot consider the resulting light curve as strictly periodic. This fact, which might be interpreted as an indication of multiperiodic variations, describes at least a transient stage of the variability pattern of this star occurred during the first observational season. It may represent therefore a further indication of non-stationary behaviour, this time on a scale of months.

### 3. Spectroscopy

In addition to the photometric data, our campaign of September 1992 yielded 50 spectrograms distributed over 4 nights with a total useful observing time of about 28 hours and a baseline of 3 days. The observations were performed using a standard *Boller & Chivens* mod. 31523 grating spectrograph equipped with a CCD detector and attached to the 2.12 m telescope of the *Observatorio Astronómico Nacional* (San Pedro Martir, BC, Mexico). The adopted configuration and observational procedure gave a wavelength resolution of  $\sim 0.8 \text{ \AA}$  with a sampling of  $\sim 0.4 \text{ \AA}$  in the range  $6510 - 6710 \text{ \AA}$ , covering both H $\alpha$  and the HeI $\lambda 6678$  line, with a signal-to-noise ratio of about 45 dB (i.e., in a linear scale, more than 30000). The images have been processed using the MIDAS package developed by the ESO.

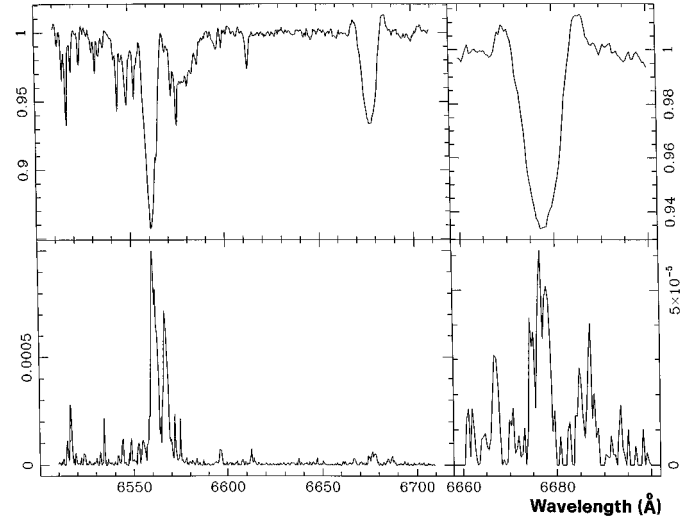


**Fig. 5.** Average of our 50 spectrograms normalized to the continuum flux (top) and variance of the corresponding signal as a function of the wavelength (bottom). The height of the main variance peak indicates variations of flux in the H $\alpha$  shell nucleus whose standard deviation exceeds the 3% of the continuum level. An enlargement of the HeI region at  $\sim 6678 \text{ \AA}$  is shown on the right

In the mean spectrum, which we show in the top of Fig. 5 normalized to the continuum flux, it is easy to identify, besides several telluric H $_2$ O lines, three components in H $\alpha$  (the photospheric line, a circumstellar emission and a shell absorption nucleus). Some circumstellar features (two emission wings and a very weak shell nucleus) seem to affect also the profile of the HeI $\lambda 6678$  line, which maintains nevertheless a basically photospheric appearance. Finally, a sharp line visible at  $\sim 6613 \text{ \AA}$  cannot

originate in the photosphere of a rapid rotating star like 14 Lac. If we identify it with the well-known FeI $\lambda$ 6609 line, we must assign to its radial velocity a value of about 200 km s $^{-1}$ . The individual normalized spectra are available in electronic form.

In the bottom of the same Fig. 5 we display, as a function of the wavelength, the variance of the time series consisting of the successive flux values (normalized to the stellar continuum) registered at each pixel. These variances have been previously purified of the white noise contributions, which have been evaluated pixel by pixel determining, like we did in the analysis of the photometric series, the root-mean-square differences between closely consecutive data. Apparently, the star shows a considerable spectral variability, which affects mainly the circumstellar components of H $\alpha$ . Moreover, the figure shows several peaks at the wavelengths of the atmospheric lines, obviously due to air mass and humidity changes, and indicates the presence of minor variations both in the peculiar line at  $\sim$ 6613 Å and in the HeI $\lambda$ 6678 profile. We can easily realize, observing the enlargement presented on the left in the same figure, that also in this line the variability seems to affect mainly the circumstellar features.

A period analysis has been performed pixel by pixel, using Vanicek's (1971) method and scanning again the frequency interval 0 – 10 d $^{-1}$ , in the ranges covered by the visible spectral lines: 6539 – 6591 Å (except the pixels corresponding to the atmospheric features) 6611 – 6616 Å and 6668 – 6689 Å. Following a procedure similar to the one introduced by Gies & Kullavanijaya (1988), in each of these three ranges we averaged the frequency spectra of the series of fluxes which describe the evolution of the line profile. Although our exiguous temporal baseline would not allow us to resolve the frequencies detected in the light curves, the resulting spectra appear consistent with the photometric time scales and lead us to rule out, also in the observed spectral variability, the presence of short period components.

The changes observed in H $\alpha$  are shown in Fig. 6, in which we can compare our nightly mean profiles. In this picture the atmospheric lines have been removed replacing, in the corresponding pixels, the observed fluxes with values obtained through linear interpolations. Everything, especially in the circumstellar features, appears to change from night to night. In order to quantify these variations, we performed for each spectrogram a nonlinear least squares fit of the H $\alpha$  profile using three gaussian curves to represent, as shown in Fig. 7, its different components. The nightly mean values of the resulting parameters are displayed in Table 5. Interested people can ask us for the complete printout. The reliability of the radial velocity data, obviously referred to the Sun, is assured by the adoption, as comparison standards, the above quoted H<sub>2</sub>O lines. The circumstellar components show the expected considerable variations, whereas minor changes in the photospheric profile must be considered dubious: they might

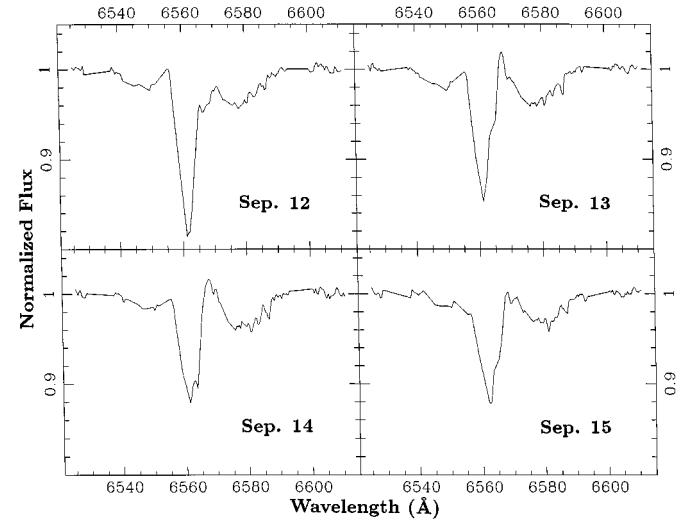


**Fig. 6.** Nightly mean profiles in the H $\alpha$  region after removal of the telluric lines. The dates are consistent with the Universal Time

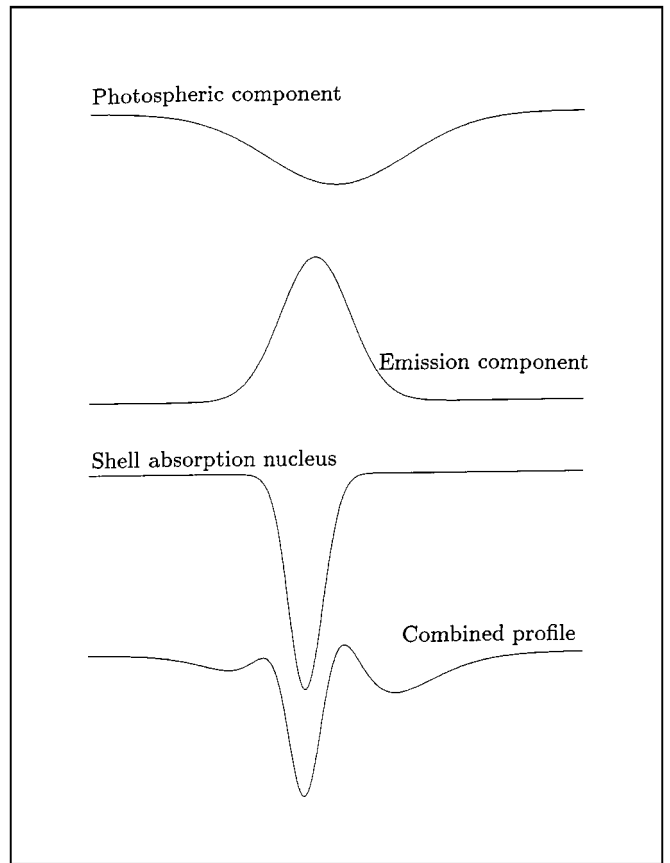


**Fig. 7.** Decomposition of the H $\alpha$  profile adopted for the quantification, displayed in Table 5, of its observed changes

**Table 5.** The observed H $\alpha$  variability described according to the decomposition of the line profile shown in Fig. 7. Conforming to the standard usage, we assign positive values to the equivalent width of the absorption components

Hel. J.D.	Component	Equiv. Width ( $\text{\AA}$ )	$\sigma$ ( $\text{\AA}$ )	Radial Vel. ( $\text{km s}^{-1}$ )
2 448 877.870	photospheric emission	$2.44 \pm .02$	$11.56 \pm .13$	134
	shell nucleus	$-1.47 \pm .05$	$7.46 \pm .17$	$3 \pm 3$
	shell nucleus	$1.03 \pm .03$	$2.29 \pm .04$	$-57$
878.821	photospheric emission	$2.39 \pm .02$	$11.23 \pm .13$	129
	shell nucleus	$-2.24 \pm .06$	$6.39 \pm .09$	$10 \pm 3$
	shell nucleus	$1.42 \pm .05$	$2.88 \pm .04$	$-66 \pm 2$
879.815	photospheric emission	$2.37 \pm .03$	$10.95 \pm .30$	134
	shell nucleus	$-2.56 \pm .06$	$5.94 \pm .11$	$11 \pm 8$
	shell nucleus	$1.62 \pm .07$	$3.15 \pm .05$	$-58$
880.757	photospheric emission	$2.37 \pm .01$	$11.03 \pm .09$	136
	shell nucleus	$-2.32 \pm .10$	$6.77 \pm .16$	$40 \pm 6$
	shell nucleus	$1.43 \pm .11$	$3.39 \pm .10$	$-36$

be produced by interference phenomena among the different components due to inadequacy of our simple fitting model.

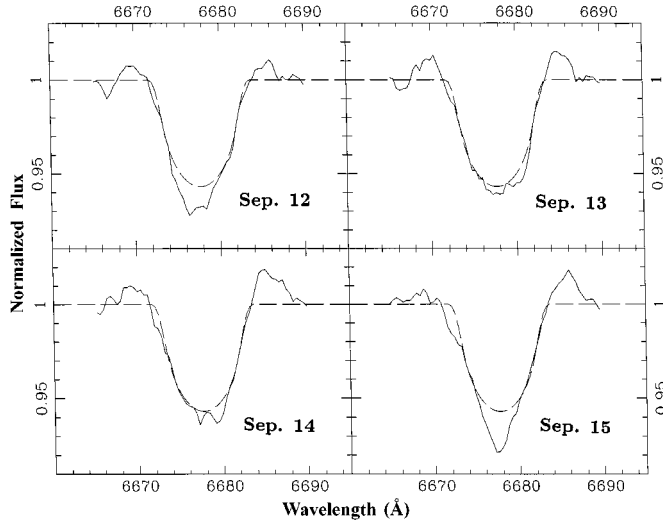


**Fig. 8.** Nightly HeI $\lambda$ 6678 mean profiles (solid lines) compared with a synthetic photospheric profile (dashed lines) corresponding to an intrinsic half-width of 1.1  $\text{\AA}$  with a Doppler broadening  $v \sin i = 220 \text{ km s}^{-1}$

The circumstellar origin of the observed variability is supported by a comparison of the HeI $\lambda$ 6678 nightly mean profiles with a synthetic photospheric profile ( $v \sin i = 220 \text{ km s}^{-1}$ ; intrinsic half-width = 1.1  $\text{\AA}$ ; equivalent width

= 0.443  $\text{\AA}$ ): the observed changes (see Fig. 8) apparently affect only the emission wings and a faint nucleus which seems to show a double core in 3 nights over 4. Our model of photospheric profile has been also combined with one (in the case of Sept. 15) or two gaussian absorption components in a nonlinear least squares fit of the central part of this line, obtaining some meaningful parameters shown in Table 6.

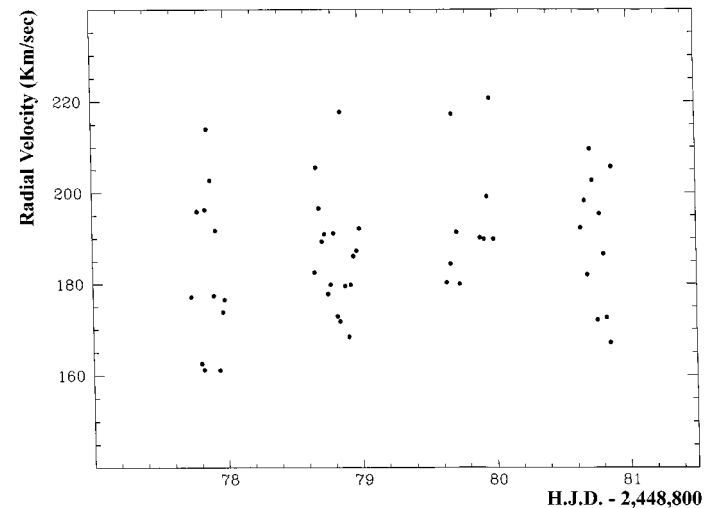


**Fig. 9.** Radial velocity curve of the sharp line visible at  $\sim$ 6613  $\text{\AA}$  in the hypothesis of its identification with the FeI $\lambda$ 6609 line

**Table 6.** Nightly mean values of equivalent width and radial velocity of the absorption components of the HeI $\lambda$ 6678 line profile

Hel. J.D.	Equivalent Width ( $\text{\AA}$ )		Radial Velocity ( $\text{km s}^{-1}$ )		
	Left Core	Right Core	Photosph. Prof.	Left Core	Right Core
2 448 877.870	$0.050 \pm .008$	$0.010 \pm .002$	$-11 \pm 3$	$-80 \pm 6$	$24 \pm 6$
878.821	$0.011 \pm .002$	$0.012 \pm .002$	$-17 \pm 5$	$-37 \pm 11$	$166 \pm 5$
879.815	$0.005 \pm .001$	$0.015 \pm .002$	$-23 \pm 6$	$-46 \pm 3$	$1 \pm 6$
880.757	$0.059 \pm .007$		$-20 \pm 4$	$-28 \pm 11$	

The poor signal-to-noise ratio does not allow us to perform a profile analysis of the sharp line at  $\sim$ 6613  $\text{\AA}$ : we can produce only its radial velocity curve (Fig. 9) and its nightly mean equivalent widths (shown in Table 7 together with the corresponding mean values of the radial velocity).

**Table 7.** Nightly mean values of equivalent width and radial velocity of the sharp line visible at  $\sim$  6613  $\text{\AA}$ 

Hel. J.D.	Equiv. Width ( $\text{\AA}$ )	Rad. Vel. ( $\text{km s}^{-1}$ )
2 448 877.870	$0.060 \pm .005$	$183 \pm 5$
878.821	$0.051 \pm .003$	$186 \pm 3$
879.815	$0.043 \pm .003$	$194 \pm 4$
880.757	$0.047 \pm .004$	$189 \pm 4$

#### 4. A double-lined binary star?

The values of mass, radius and effective temperature of a non-rotating B4 III star are of about  $7.7 M_{\odot}$ ,  $7.5 R_{\odot}$  and 16000 K respectively. 14 Lac is, however, a rapidly rotating object. The presence of a strong shell feature in H $\alpha$  involves an almost equator-on view and, therefore, a rotational displacement quasi-parallel with the main sequence towards cooler and fainter areas in the HR diagram (see e.g. Maeder & Peytremann 1972). A B3 IV star ( $M \simeq 8 M_{\odot}$ ), rotating with the estimated equatorial velocity of  $220 \text{ km s}^{-1}$ , would reproduce quite well the observed parameters. Polar and equatorial radii and temperatures of such a body can be estimated to be respectively  $R_p \simeq 7 R_{\odot}$ ,  $R_e \simeq 7.8 R_{\odot}$ ,  $T_p \simeq 17900 \text{ K}$  and  $T_e \simeq 15\,700 \text{ K}$ .

In the binary hypothesis we can evaluate, assuming circular orbits, the velocities of the components:

$$v(\text{Be}) = m \left( \frac{2\pi G}{P(M+m)^2} \right)^{\frac{1}{3}};$$

$$v(\text{companion}) = \frac{M}{m} v(\text{Be}), \quad (1)$$

where  $P$  is the orbital period,  $M$  and  $m$  the masses of the Be and of the companion star respectively. If we assume  $M \simeq 8 M_{\odot}$  and  $P \simeq 10$  days, one of these orbital velocities must exceed  $125 \text{ km s}^{-1}$ . Considering that, as we have only just seen, the angle between the view line and the orbital plane couldn't be too wide, we are assured by expressions (1) that or the Be star or the companion would show radial velocity variations of at least  $200 \text{ km s}^{-1}$  in the  $\sim 10^d$  period. Our  $\sim 3^d$  baseline reduces these minimum changes to values which range, according to the location of the observational window, from  $\sim 40$  to  $\sim 160 \text{ km s}^{-1}$ . Nothing like this is visible in the spectrum of the primary star: the nightly mean velocities reported in Table 5 and in Table 6 for the H $\alpha$  and the HeI $\lambda$ 6678 photospheric component respectively show no significant variation. Therefore we have to look for a low mass companion. The sharp line visible at  $\sim$ 6613  $\text{\AA}$  cannot be ascribed to it: its observed radial velocity, as reported in Table 7 and shown in Fig. 9, appears constant within the error bars.

Only the double-core HeI $\lambda$ 6678 profile could result from a combination of three different sources and indicate the presence of a binary system. Obviously, the wide component dashed in Fig. 8 originates in the photosphere of the Be star. The left absorption feature, whose intensity shows in Table 6 considerable changes, is produced without doubt, as well as the emission wings, in the circumstellar region. Finally, the right absorption nucleus, which seems to conserve a constant equivalent width of about 0.012  $\text{\AA}$  and exhibits large radial velocity variations, could represent the signature of the secondary body. The low mass assignable to this object does not cause problems in principle: cool stars present a FeI line at almost the same wavelength (it is easy to get the corresponding

radial velocities adding  $\sim 7 \text{ km s}^{-1}$  to the values presented in Table 6)

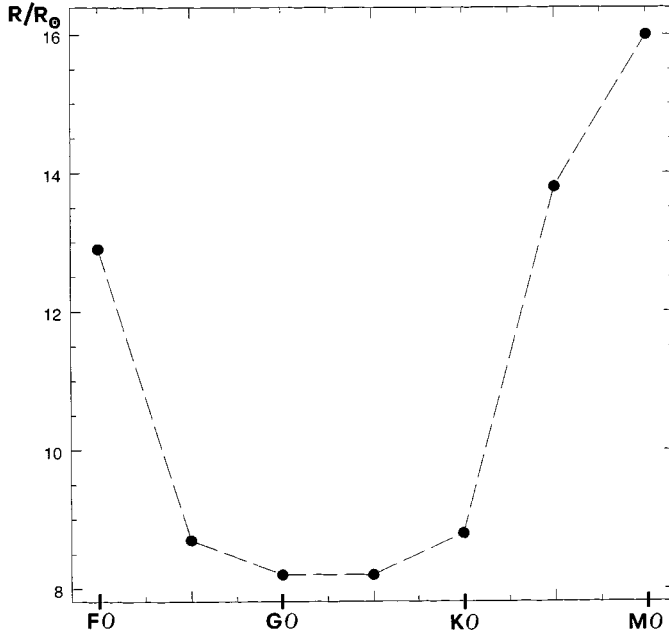


**Fig. 10.** Radius of the secondary star (in solar units) required in the binary hypothesis to reproduce the observed FeI $\lambda 6678$  absorption intensity as a function of its spectral type

This model meets no difficulties in passing a first quantitative examination. The equivalent width which a feature belonging to the spectrum  $c$  of the companion would present if observed in the combined spectrum  $B + c$  is:

$$EW_{B+c} \simeq \frac{EW_c}{1 + \frac{R_B^2}{R_c^2} \frac{e^{\frac{hc}{k\lambda T_c}} - 1}{e^{\frac{hc}{k\lambda T_B}} - 1}}, \quad (2)$$

where  $EW_c$  is the corresponding equivalent width in the spectrum  $c$ ,  $R_B$ ,  $R_c$ ,  $T_B$  and  $T_c$  radii and temperatures respectively of  $B$  and of the companion star,  $\lambda$  the wavelength of the observed feature. Equation (2) allows us to evaluate the radius of the secondary star required to reproduce the observed FeI $\lambda 6678$  absorption intensity. The result, shown in Fig. 10 as a function of the spectral type, would be consistent with the geometry of the system: assuming mass values of  $\sim 8$  and  $\sim 1 M_\odot$  for the primary and the secondary body respectively, we get an orbital radius of  $\sim 41 R_\odot$  and a distance of  $\sim 12.5 R_\odot$  between the barycenter of the companion star and the Lagrangian point L<sub>1</sub>. Also the radial velocity variations which appear in Table 6 are in agreement with the orbital velocity of  $\sim 180 \text{ km s}^{-1}$  resulting from Eq. (1) for the secondary stars.

Of course, we can have our reservations about the high eccentricity which would be entailed by the observed velocity pattern, but we must consider that this pattern is defined by four points only, the last of which, moreover, is perturbed by a blending effect with a circumstellar feature. This consideration, on the other hand, makes us cautious about claiming conclusive evidence of duplicity, and justifies our question marks.

## 5. Circumstellar origin of the double-wave variations

The ellipsoidal model suggested for this star by Hill et al. (1976) must be ruled out on the grounds of two strong pieces of evidence: the dramatic changes shown by the light curves from 1969 to 1992 and the light-colour correlations obtained just from the data presented by these authors. In a short period binary star, the tidal strain cannot disappear for years, yielding the flat light curve observed by Garrido et al. (1983), and then become again visible. On the other hand, an ellipsoidal variable would appear redder at the light minima than at the light maxima: the effective temperature in two arbitrary points on the surface of a distorted star in radiative equilibrium fulfills the relation  $T_1/T_2 \simeq (g_1/g_2)^{\frac{1}{4}}$ , where  $g_1$  and  $g_2$  are the respective gravity values. The heating produced by the presence of the companion (often misleadingly called *reflection effect*) can cause changes only on the side facing the secondary component. The contrary follows from the colour curves obtained from Dominion's simultaneous multifilter measurements. In Fig. 11 we can compare a light curve ( $\Delta(55)$ , in the top of the figure) with a colour curve ( $\Delta((44) - (55))$ , in the middle), both phased with the previously determined frequency of  $0.09918 \text{ d}^{-1}$ : luminosity and colour temperature increase upwards. The periodic component of the  $\Delta((35) - (44))$  curve (bottom of the figure), which has been isolated resorting again to the MPDM method (Bossi & La Franceschina 1995), shows an intermediate phase shift.

The negative correlation which we observe between luminosity and colour temperature could in principle be consistent with an eclipsing binary mechanism. It would entail an eclipsing body hotter than the eclipsed one both in the primary and in the secondary light minimum; however, the strong rotational distortion of the Be object could make it plausible at first glance: a companion with an intermediate temperature between the equatorial belt of the primary star and the average of its projected figure, if put into an *ad hoc* orbit, would meet this requirement. Nevertheless, a quantitative model fitting proves a hopeless task: the temperature range on the surface of 14 Lac, as it has been evaluated in the preceding section, is very far from explaining the colour variations implied by the data of Hill et al. (1976). Moreover, a comparison of the equatorial radius to the orbital separation leads us to exclude a simple succession of eclipses as the mechanism

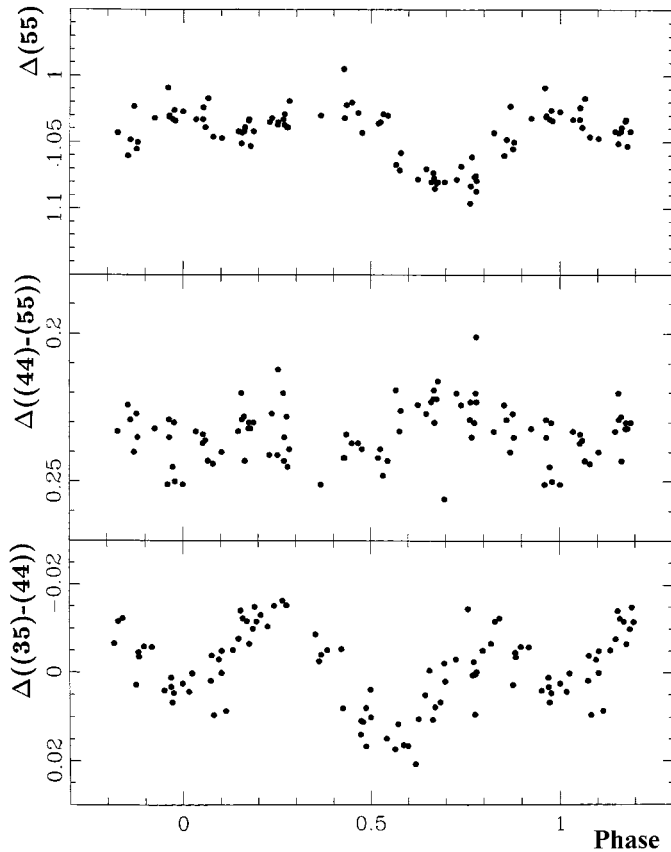


**Fig. 11.**  $\Delta(55)$  light curve (top),  $\Delta((44)-(55))$  colour curve (in the middle) and periodic component of the  $\Delta((35)-(44))$  curve (bottom). All these series of data, obtained from the photometry published by Hill et al. (1976), are phased with a frequency of  $0.09918 \text{ d}^{-1}$ . Luminosity and colour temperature increase upwards

responsible of the observed light changes. On the other hand, the absence in the light curves of horizontal stretches between eclipses cannot be due to the tidal strains: as stated above, it would not agree with the observed light–colour correlations. Besides, we can neglect the effect of tidal strains on the basis of simple dynamical considerations. The upper limit of the gravity perturbation due to tide is given by the expression:

$$\lim_{m \rightarrow \infty} g_t = \lim_{m \rightarrow \infty} 8\pi^2 \frac{m}{M+m} \frac{R_e}{P^2} = 8\pi^2 \frac{R_e}{P^2} .$$

We can easily verify that, assuming  $P \simeq 10$  days, not even the presence of a supermassive black hole would cause at the equator of 14 Lac more than a  $\sim 2\%$  gravity perturbation.

The fraction of the total measured  $V$  light ascribable to a secondary star whose radius fulfils Eq. (2) is shown in Fig. 12. As can be immediately realized, only the tidal deformation of an F0 companion could in theory reproduce the scale of the observed variations. Another strong

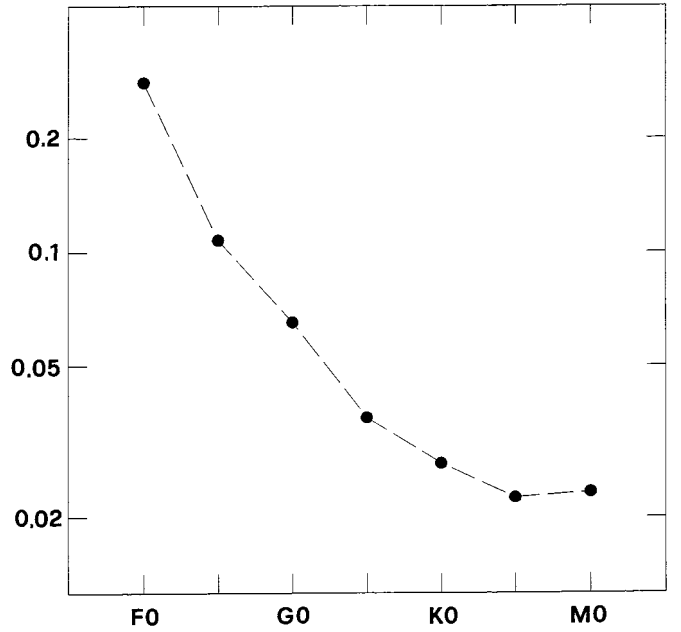


**Fig. 12.** Fraction of the total measured  $V$  light ascribable to a secondary star whose radius fulfils Eq. (2) as a function of its spectral type

constraint must be laid down on the angle  $\alpha \simeq \frac{\pi}{2} - i$  between the view line and the orbital plane: small values ( $\alpha < \sim 30^\circ$ ) would result in deep eclipses (up to  $\sim 1^{m}4$  in  $V$ ), high values ( $\alpha > \sim 45^\circ$ ) would reduce both the rotational luminosity modulation of the secondary body and the projected component of its orbital motion below the observed thresholds. In spite of these narrow boundaries, the assumption of a strongly deformed companion as the source of the light variations would have the advantage of an at least qualitative consistency with our light–colour correlations: such object would contribute the  $\sim 28\%$  of the total  $V$  light against the  $\sim 19\%$  and the  $\sim 11\%$  of the  $B$  and  $U$  lights respectively. Nevertheless, also this variant of the ellipsoidal model is ruled out by the observations of Garrido et al. (1983). In fact, if we combine the photometry presented by these authors with our spectroscopy, we are led to assign the companion star to a spectral type not far from K0.

If the light curve of 14 Lac proves inconsistent with simple duplicity effects, it seems to make up for it correlating with the considerable changes shown in the same time scale by all the circumstellar components of our spectra, including the very peculiar line visible at  $\sim 6613 \text{ \AA}$  (as we have seen, it can neither originate in the photosphere of the  $B$  star nor belong to the spectrum of a companion): in Fig. 13 our  $\Delta V$  curve is compared to the nightly mean intensities of these features. Therefore, nothing remains except for us to ascribe the variability observed in this star to circumstellar phenomena. Moreover, our data indicate a complex shell structure: to the light decrease

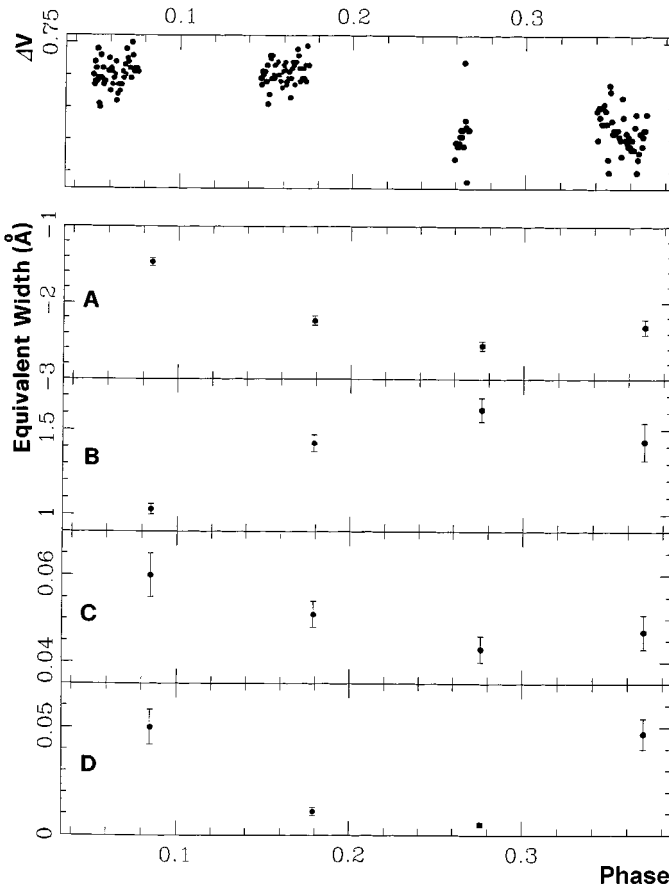


**Fig. 13.** Our  $\Delta V$  curve (top) compared to the nightly mean intensities of the  $H\alpha$  emission component **A**), of the  $H\alpha$  shell nucleus **B**), of the ( $FeI?$ ) line visible at  $\sim 6613 \text{ \AA}$  **C**) and of the probable  $HeI\lambda 6678$  shell nucleus **D**). All the data are phased with a frequency of  $0.0982 \text{ d}^{-1}$

during the secondary minimum corresponds an intensity rise of the circumstellar  $H\alpha$  components, while the line at  $\sim 6613 \text{ \AA}$  and the  $HeI\lambda 6678$  shell nucleus undergo simultaneous intensity falls.

This result does not diminish the relevance of a probable duplicity. As can be clearly seen, duplicity is likely to play an important rôle in the modulation of the circumstellar effects: the gravitational perturbation due to the presence of a second body breaks any symmetry in the envelope of a shell star causing observable changes characterized by its orbital period.

## 6. Open problems

All our evidence of duplicity lies in four measurements of an hardly perceptible spectral feature. Maybe the answer to all our problems will be contained in the above mentioned paper announced by Pavlovski et al. (1994). Anyway, awaiting further pieces of information, we can suggest (to ourselves as well as to the readers) that the observation of some select spectral regions would be in

principle a conclusive test. In particular, the presence of a secondary star like the one hypothesized in Sect. 4 would be betrayed by the CaII K and H doublet: the CaII K equivalent width in the combined spectrum would range between  $\sim 0.07 \text{ \AA}$  (M0 type companion) and  $\sim 0.4 \text{ \AA}$  (G0). If the secondary body was a late type giant, also the observation of the MgI  $\lambda 5173$  and  $\lambda 5184$  doublet would allow us to detect easily its presence.

Do to the non-standard variability pattern shown by this star, both a possible refutation and a confirmation of the binary hypothesis would hold the greatest interest for us.

We are observing a light curve which differs from the ones exhibited by many Be stars, according to Balona and co-workers (see e.g. Balona et al. 1987, or van Vuuren et al. 1988), only in its atypical period. We meet, as these authors do, almost the same frequency in different years, whereas shape and amplitude of the signal show considerable variations. Also the double-wave pattern observed in this star would fit their scenario. If 14 Lac belongs to a close binary system, these similarities may represent the fortuitous outcome of two distinct mechanisms: orbital and rotational modulation respectively. Otherwise, if we consider this star as a normal Be object, we have to look for other models accounting for the same peculiar kind of variability in all the observed time scales: in 14 Lac it cannot be ascribed, as in the above quoted papers, to systems of spots carried around the star by its rotation (the entailed equatorial radius of not less than  $\sim 44 R_\odot$  would not be credible).

In the binary hypothesis, we got indications of a strongly eccentric orbit which hold our attention to the probable youth of the system: the evolutionary status of the Be stars is still unknown. On the other hand, the observation of an orbital period which is really increasing would puzzle us very much: neither tidal frictions nor realistic mass transfer phenomena seem to be able to account for our estimate of the increase rate (more than 1% in 20 years). Obviously, also this scenario would need some checks: a spectroscopic monitoring of the whole  $\sim 10$  d period would give us useful bits of information about the orbital parameters, whereas an extended photometric baseline would reduce the error in our period determinations, allowing us to verify reality and rate of the observed secular frequency trend.

For these reasons we included 14 Lac in a list of few selected Be stars to be observed in the next seasons. Proposals of collaboration would be welcome.

*Acknowledgements.* We are grateful to L. Mantegazza and M. Rodonò for allowing us to use their unpublished photometry in the present work. Thanks are due also to the referee, P. Harmanec, which called our attention to the possible binary nature of our  $HeI\lambda 6678$  spectral line.

## References

- Andrews P.J., 1968, MNRAS 72, 35  
 Balona L.A., Marang F., Monderen P., Reitermann F., Zickgraf F.J., 1987, A&A 71, 11  
 Bossi M., La Franceschina L., 1995, A&AS 113, 387  
 Garrido R., Sareyan J.-P., Gimenez A., Valtier J.-C., Delgado A.J., le Contel J.-M., Ducatel D., 1983, A&A 122, 193  
 Gies D.R., Kullavanijaya A., 1988, ApJ 326, 813  
 Goraya P.S., Gurm H.S., 1987, A&A 180, 167  
 Hill G., Hilditch R.W., Pfannenschmidt E.L., 1976, Publ. Dom. Astr. Observ. 15, 1  
 Maeder A., Peytremann E., 1972, A&A 21, 279  
 Mantegazza L., 1980, Inf. Bull. Variable Stars 1886  
 Mantegazza L., 1995 (private communication)  
 Pavlovski K., Božić H., Ružić Ž., Harmanec P., Horn J., Koubský P., Juza K., Hadrava P., Kříž S., Štefl S., Ždářský F., 1994, in Pulsation, Rotation and Mass Loss in Early-Type Stars, IAU Symposium 162, Balona L.A., Henrichs H.F. and le Contel J.-M. (eds.). Kluwer Academic Publishers, Dordrecht, Holland, p. 301  
 Poretti E., Zerbi F.M., 1993, A&A 268, 369  
 Richardson E.H., 1977, Q. J. R. Astr. Soc. 18, 382  
 Simon N.R., Lee A.S., 1981, ApJ 248, 291  
 Slettebak A., 1982, ApJS 50, 55  
 Stellingwerf R.F., 1978, ApJ 224, 953  
 Uesugi A., Fukuda I., 1982, Revised Catalogue of Stellar Rotational Velocities, Deptt. Astron. Kyoto University, Kyoto, Japan  
 Vanicek P., 1971, ApSS 12, 10  
 van Vuuren G.W., Balona L.A., Marang F., 1988, MNRAS 234, 273  
 Wackerling L.R., 1970, PASP 82, 1357  
 Walker M., 1952, ApJ 116, 106